A Wind-Tunnel Technique for Measuring Frequency-Response Functions for Gust Load Analyses

JEAN GILMAN JR.* AND ROBERT M. BENNETT†
NASA Langley Research Center, Hampton, Va.

A technique for experimentally evaluating the frequency-response functions of a flexible airplane to vertical sinusoidal gusts is described. It consists of measuring the response of an aeroelastically scaled model in simulated free flight to a gust field generated in a wind tunnel by oscillating airfoils located upstream of the test section. Freedom of the model in an approximation of free flight is provided by a two-cable support system developed previously for flutter research. The airstream oscillator system is described, and the model mount system is described and analyzed. Some results of an application to a fighter-type model are presented. From the initial results it appears that a means of generating an oscillating airstream of sufficient strength and uniformity for useful gust research has been developed. The analysis of the two-cable mount system shows that with proper design the free-flight frequency-response function for the rigid body modes can be simulated satisfactorily. Application to a fighter-type model illustrates that useful results can be obtained.

Nomenclature

$\bar{c}$ = mean aerodynamic chord, ft
C_D = drag coefficient, drag/qS
C_L = lift coefficient, lift/qS
C_{L_α} = $\partial C_L/\partial\alpha$
C_m = pitching-moment coefficient, pitching moment/$qS\bar{c}$
C_{m_q} = $\partial C_m/\partial(\dot{\theta}\bar{c}/2V)$
C_{m_α} = $\partial C_m/\partial\alpha$
$C_{m_{\dot{\alpha}}}$ = $\partial C_m/\partial(\dot{\alpha}\bar{c}/2V)$
C_n = normal-force coefficient, $m\ddot{z}/(qS)$
C_{BM} = wing bending-moment coefficient, bending moment/$(qS\bar{c})$
d_z = distance from the vane quarter chord to point of reference in test section
f = frequency, cps
g = acceleration due to gravity
I_y = moment of inertia about pitch axis, slug/ft^2
k = reduced frequency, $\bar{c}\omega/(2V)$
k_{zz}, $k_{z\theta}$, $k_{\theta\theta}$ = mount system stiffness influence coefficient giving increment in cable restraining forces or moments in coordinate i due to unit deflection in coordinate j; $i, j = z$, and θ
m = mass, slugs
M = Mach number
q = dynamic pressure, lb/sq ft
r_y = radius of gyration about pitch axis, $(I_y/m)^{1/2}$, ft
S = wing area, ft^2
T_R = rear-cable tension, lb
V = velocity, fps
W = weight, lb
y = lateral displacement coordinate, ft
z = vertical displacement coordinate, ft
α = angle of attack
ϵ_g = angle of gust with respect to tunnel centerline
ζ_z, ζ_θ = effective viscous damping ratio of mount system for no-wind condition in mode z and θ, respectively
θ = pitch angle
θ_v = pitch-amplitude angle of oscillator vanes
σ = $\rho VS/(2m)$
φ = phase angle
φ_g = phase angle of gust at point of reference with respect to vane position
ω = circular frequency, rad/sec
ω_p = circular frequency of plunging mode, rad/sec
$\dot{}$ = dot over variable indicates d/dt

Presented as Preprint 65-787 at the AIAA/RAeS/JSASS Aircraft Design and Technology Meeting, Los Angeles, Calif., November 15–18, 1965; submitted January 24, 1966; revision received May 11, 1966.

* Aerospace Engineer.
† Aerospace Engineer. Member AIAA.

Introduction

ATMOSPHERIC gust loads are an important aircraft design consideration since they affect structural design loads, structural fatigue life, and pilot fatigue. They may be particularly pronounced for a low-altitude, high-speed mission, or for very large flexible aircraft with low natural frequencies. Methods of determining the response of aircraft to random atmospheric gusts or turbulence have been developed based on power spectral analysis techniques (for example, see Ref. 1). An essential element of these analyses is the response of the flexible airplane to excitation by sinusoidal gusts, or the frequency-response function. In the past, these frequency-response functions have been obtained from flight-test data by inference from measured gust inputs and aircraft response, or from analytical methods (Refs. 2 to 5). However, the aeroelastician may be faced with odd or unusual designs out of the realm of past experience, or with areas for which analytical procedures may be undeveloped or unreliable, such as the transonic range. Thus, a method for experimentally evaluating the frequency-response function under controlled conditions during the design stages is desired. This paper describes some progress in development of a wind-tunnel technique for this purpose.

The technique consists of measuring the response of an aeroelastically scaled model to an oscillating vertical gust field generated in the Langley transonic dynamics tunnel by oscillating vanes located upstream of the test section. The model is flown on a cable support system which permits simulation of the free-flight modes of motion. This paper gives a description of the oscillator system and the model mounting system, a discussion of some aspects of their design, and illustrates their application to a fighter-type airplane model.

Description of the Airstream Oscillator

In the development of the airstream oscillator, primary emphasis has been placed on the generation of a nearly one-dimensional gust field in the test section. Thus the requirements are that the oscillating airstream must be of nearly constant amplitude and in phase over a sufficiently large portion of the test section to immerse a model of reasonable

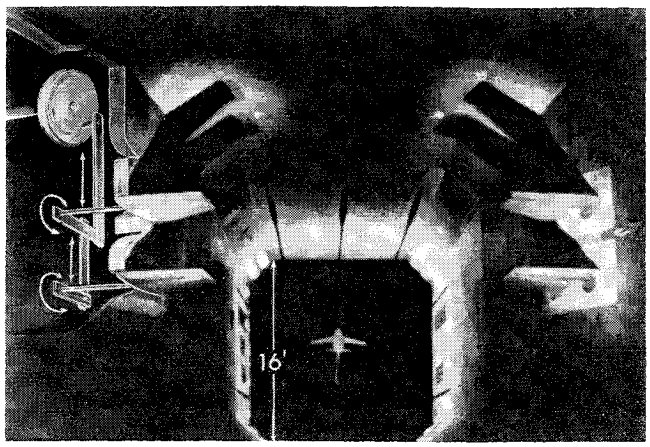

Fig. 1 Photograph of vanes and model in the Langley transonic dynamic tunnel showing cutaway of mechanism.

size, such as a 6-ft-span model. The amplitude also must be of sufficient strength to be discerned from wind-tunnel turbulence and to provide sufficiently large excitation to the model for accurate response measurements.

Interest in oscillating an airstream in this fashion has existed for several years. Some early tests[6] were attempted using a two-dimensional plunging airfoil upstream of the test section. However, the magnitude of the airstream oscillation was small, and difficulty was encountered in distinguishing it from tunnel turbulence. The present design is based on the use of the vertical component of the trailing tip vortex system behind moderate aspect ratio bi-plane vanes. A pilot model of this concept was tested in the Langley low-turbulence tunnel. The results[7] indicated that airstream angles of the order of 15% of vane angle and a region of nearly constant amplitude and phase could be obtained over about 20% of the tunnel width. On the basis of these results, the present oscillator was constructed for the Langley transonic dynamics tunnel. With the airstream oscillator in this tunnel, the particularly difficult transonic gust loads problem can be investigated in a facility specifically designed for aeroelastic testing. The tunnel has a square, 16-ft, slotted test section and is capable of testing at Mach numbers up to 1.2 in air or freon-12 over a wide range of densities.

The installation of the vanes in the tunnel is shown schematically in Fig. 1. A set of biplane vanes are located on each wall in the converging subsonic portion of the entrance nozzle of the tunnel. The vanes are 3.5 ft in span, and have a taper ratio of 0.5 and a panel aspect ratio of 1.2. The two vanes of a biplane set are linked mechanically, and the biplanes are oscillated about the quarter chord by means of hydraulic motors driving a large flywheel with an offset linkage. Each set of biplanes is driven independently, and control and synchronization are maintained by electronic controls.

The oscillator system was designed for long duration operation at preset vane amplitudes from 3° to 12° and at frequencies up to 20 cps. The higher frequencies and amplitudes result in a severe loads problem on the vanes which was minimized by lightweight construction. The design uses a built-up steel spar, an aluminum honeycomb core, and a laminated fiberglas skin. Currently, operation is power limited as a result of the power absorbed by aerodynamic damping of the vanes. This power limitation gives a frequency limit as a combination of vane angle and dynamic pressure. For a 20-cps operation, the limit varies from a dynamic pressure of about 60 lb/ft² at 12° vane amplitude to about 350 lb/ft² at 3° vane amplitude. This latter value is near the maximum dynamic pressure capability of the tunnel in the transonic Mach number range.

Some results of an initial airstream calibration are presented in Figs. 2 to 4 as measured by differential pressure flow-angle probes. The results for the tunnel centerline are summarized in Fig. 2 for several Mach numbers. The amplitude gradually decreases with frequency, and the phase angle varies essentially with the fraction of the wavelength from the vanes to the point of measurement (49 ft from the vane quarter chord to point of measurement in this case). These data are based on 1-min averages of the output of an electronic sine-cosine resolver system that gives the in-phase and out-of-phase components of the first harmonic of stream angle with respect to vane position. This procedure tends to average out the effect of tunnel turbulence.

An example of the horizontal distributions across the center of the tunnel of gust amplitude and phase angle is given in Fig. 3 for a Mach number of 1.0. Although the resolution of amplitude is only about 0.1°, the trend of amplitude and phase angles appears in many cases to indicate a sufficiently constant region for the testing of a 6-ft-span model; however, in other cases there would be considerable amplitude variation across the span. Further work is needed to define the conditions where these nonuniform regions occur.

The horizontal centerline lateral distributions of Fig. 3 are compared with data for 2 ft above and below the centerline in Fig. 4. The data indicate that there is some variation in amplitude off the centerline, but these differences are not large except outboard of 3 ft from the centerline where rapid variations take place. Thus, from these initial calibra-

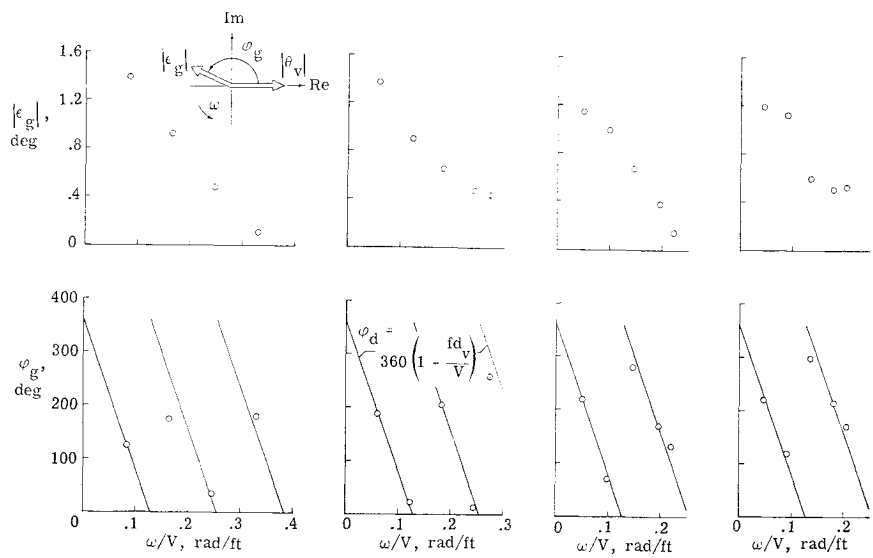

Fig. 2 Variation of gust amplitude and phase angle at the tunnel centerline with wavelength parameter; $\theta_v = 9°$; a) $M = 0.27$ in air, b) $M = 0.80$ in freon, c) $M = 1.00$ in freon, d) $M = 1.10$ in freon; (left to right).

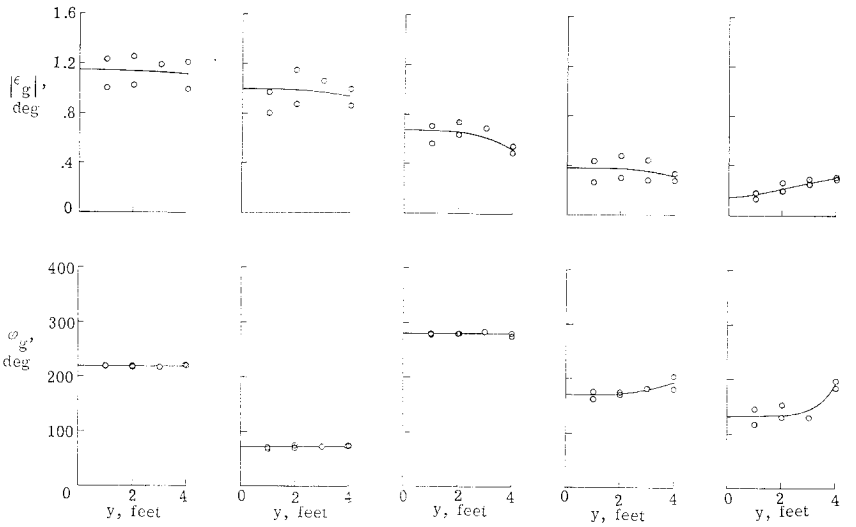

Fig. 3 Lateral distribution across the tunnel centerline of gust amplitude and phase angle for a Mach number of 1.00 in freon; $\theta_v = 9°$; a) $\omega/V = 0.049$ rad/ft, $f = 4$ cps; b) $\omega/V = 0.098$ rad/ft, $f = 8$ cps; c) $\omega/V = 0.146$ rad/ft, $f = 12$ cps; d) $\omega/V = 0.196$ rad/ft, $f = 16$ cps; e) $\omega/V = 0.219$ rad/ft, $f = 18$ cps; (left to right).

tion results it appears that a usable gust field of nearly 6 ft in width and 4 ft in depth is being generated.

Model Mount System

In order to obtain valid frequency-response measurements, the model must be flown in the wind tunnel with sufficient freedom that free-flight rigid-body motions are simulated. For the longitudinal case under consideration, this implies that the short-period mode of the airplane must be reproduced as accurately as possible. The mount system used for this purpose is one that has been developed for flutter research.[8] For a flutter model, the criteria that have been used generally are that the model must be stable on the mount system, and all rigid-body modes must be well separated from the structural modes of interest. However, for a gust loads model, not only must stability be achieved, but the distortion of the short-period frequency-response function by the mount must be minimized.

The mount system is shown schematically in Fig. 5. It consists of two cable loops, one loop extending upstream with its ends fixed to the floor and to the ceiling, and the other loop extending downstream with its ends fixed to the side walls. The cable loops pass through pulleys located in the fuselage, and are kept under tension by stretching a soft spring in the rear cable. In addition, a snubber cable system is provided for emergency restraint. It consists of three or four cables fastened to the model which are normally slack and extend out through the tunnel walls to a shock absorber system and a remotely operable actuator.

The cable mount system in effect adds external pitch and vertical translation springs to the model along with coupling between pitch and translation if the center of gravity of the model is not coincident with the effective elastic axis. These springs alter the short-period mode somewhat and introduce an additional low-frequency plunging mode. The effects depend on the pulley locations, cable arrangement, cable tension, and the basic stability of the model. These variables provide for considerable latitude in designing the mount to obtain desired results.

One criterion for small distortion of the short-period mode is that the frequency of the plunging mode should be separated as far as practical from the short-period frequency. An approximation to the frequency of the plunging mode is derived in Appendix B and shown as follows:

$$\omega_p^2 = (k_{zz}/m)\{1 - (k_{z\theta}/k_{zz})[qSC_{L\alpha}/(k_{\theta\theta} - qS\bar{c}C_{m_\alpha})]\} \quad (1)$$

A practical approach for keeping this frequency low is to make the pitch-plunge coupling ($k_{z\theta}$, which is normally negative) zero by locating the elastic axis at the center of gravity of the model. If the frequency is sufficiently low, then this mode can be ignored for test purposes and attention devoted to higher modes of interest.

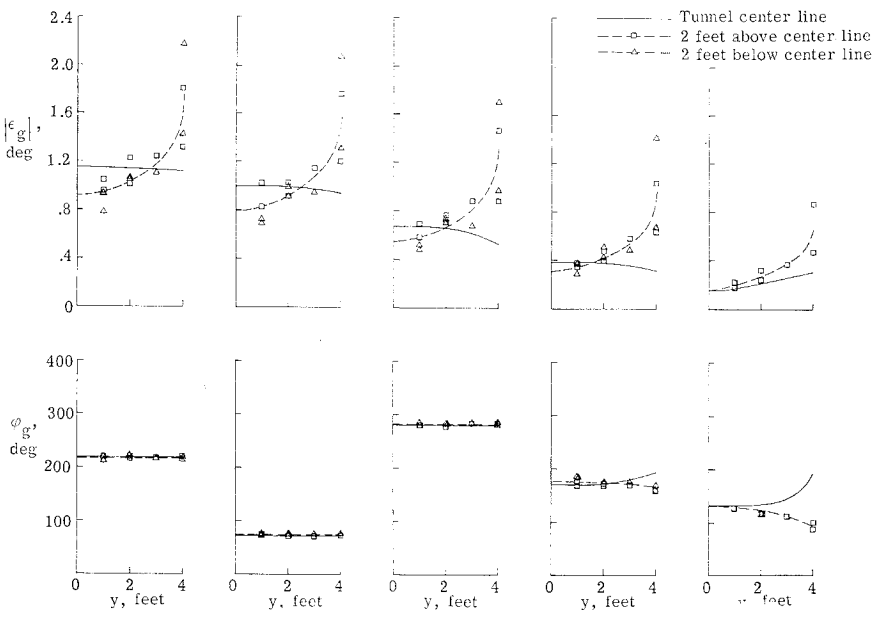

Fig. 4 Comparison of lateral distributions of gust amplitude and phase angle at the tunnel centerline and at 2 ft above and 2 ft below the tunnel centerline; Mach number of 1.00 in freon; $\theta_v = 9°$; a) $\omega/V = 0.049$ rad/ft, $f = 4$ cps; b) $\omega/V = 0.098$ rad/ft, $f = 8$ cps; c) $\omega/V = 0.146$ rad/ft, $f = 12$ cps; d) $\omega/V = 0.196$ rad/ft, $f = 16$ cps; e) $\omega/V = 0.219$ rad/ft, $f = 18$ cps; (left to right).

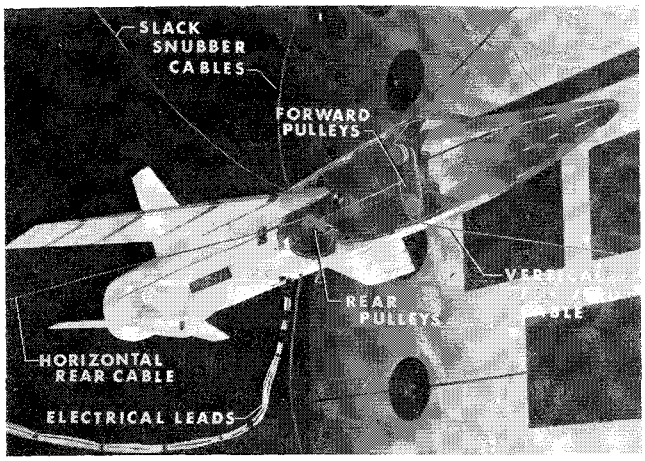

Fig. 5 Fighter-type model on the two-cable mount.

To illustrate the effect of the mount system on the frequency response, calculations using the analysis developed in Appendix A have been made for the model tested in the present program. This model has a short-period mode that is well separated from the wing modes as is subsequently described. Stability derivatives have been estimated from wind-tunnel force tests of a similar model. The calculated frequency-response function for the free-flight short-period mode (assuming constant forward velocity) is compared in Fig. 6 with those for the model for two arrangements of the mount system. For configuration A (the present test configuration), the rear pulleys are located at the center of gravity, and the ratio of cable tension to weight, T_R/W, is 1.7. For configuration B, the pulleys are shifted such that the effective elastic axis is coincident with the model center of gravity, and T_R/W has been reduced to 0.5. It is apparent that distortion of the frequency response is less for configuration B, and approaches the free-flight case. For both configurations the phase at low frequencies differs from free flight, and at zero frequency differs by 90°. However, this difference occurs over a small range of frequencies that are of little interest from the loads standpoint, and the phase could be estimated in this range if necessary. The examples presented are for Mach number 1.0 where the model has a large static margin. At lower Mach numbers, with a low static margin, the results for configuration B are similar, but for configuration A the vertical translation mode considerably distorts the short-period response.

From this analysis, it is apparent that the mount system can be designed to reproduce the short-period stability mode within reasonable tolerances, and thus can be used for valid

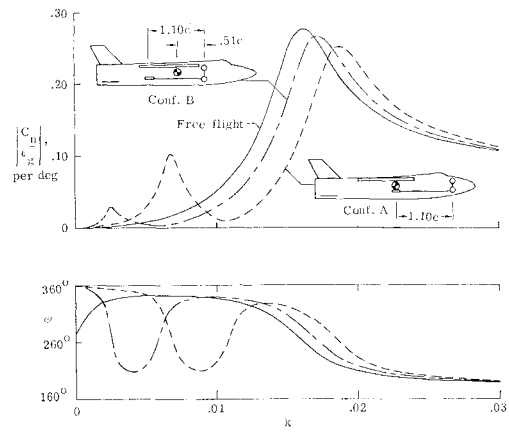

Fig. 6 Theoretical effect of the mount system on the frequency response functions for fighter-type model at $M = 1.0$.

frequency-response measurements. Furthermore, it is believed that analytical corrections could be made for the small effects of the mount system on the data near the short-period mode.

Example of Application

Some initial tests were made with a flexible model to develop instrumentation techniques, testing procedures, and data reduction procedures; to investigate model flying qualities in such a gust field; and to determine if adequate excitation was available. The model (sketched in Fig. 5) was an available model initially designed for generalized flutter research. Lead weights were added to the wings to reduce the first bending frequency of about 32 cps to about 16 cps, well within the 20-cps frequency range of the oscillator. For the test conditions, the short-period frequency of 2.4 cps was well separated from the wing bending frequency (about 16 cps). The model was instrumented with accelerometers at the center of gravity and a forward position in the fuselage, with strain gages near the wing root, and with a fast response differential pressure nose probe (geometrically similar to that of Ref. 9). Oscillator vane positions and frequency were measured also. All data were recorded on magnetic tape for later data handling.

Some initial difficulty in model flying was experienced during the starting of the vanes at an amplitude angle of 9° at low Mach numbers, as the stream angles produced at very low frequencies resulted in very large displacements. A satisfactory procedure for testing in the higher frequency range was to start the vanes oscillating at a frequency between wing bending and the short period, and then bring the tunnel up to speed. Using this procedure the model flew very well. At higher Mach numbers, where the plunging mode was damped more heavily, and with vane amplitude reduced to 6°, the vanes could be started or stopped without excessively large displacements. Use of the snubber cable system, however, provides additional assistance in starting at the higher vane amplitudes. Thus, it appears that although there can be detail problems, in general, little difficulty is experienced in flying a model on the mount system in the gust field.

The proper definition of the frequency-response function requires many points with very small increments in frequency. Taking all the necessary data at constant frequency would require considerable testing time. A procedure that has evolved and appears to give satisfactory results in a reasonable length of time is to take data points at constant frequency and also to take data continuously while proceeding from point to point using a low sweep rate. The proper sweep rate for quasi-steady data handling can be estimated from Ref. 10.

Some sample results at a Mach number of 1.0 are presented in nondimensional form in Figs. 7 and 8. The vane amplitude was 6° for these tests. The data were reduced by means of the resolver system as described previously in the airstream calibration tests. The stream angle ϵ_a for normalization of the data was taken from a smooth fairing of the points of Fig. 2c multiplied by the ratio of the vane angles. The stream-angle measurements made on the model were not usable, as the effects of model motion could not be resolved. This resulted from an inadequate measurement of pitch angle which was based on the difference in two accelerometers. In this case the accelerometers were located too close together. Good definition of the response function was obtained near the short-period mode (k of 0.021), and the presence of the plunging mode (k of 0.007) was indicated. These results indicate that the excitation and technique are adequate at low frequencies. Good excitation of the wing first bending mode is apparent also in the bending moment measurements (k of 0.151). However, the acceleration response increases unexpectedly at high k values (Fig. 8). This increase is con-

sidered to be a lack of definition in the stream-angle amplitude, as the fairing of the flow-angle data (Fig. 2c) in this region depended on a few widely separated points. There are also several dips that are noticeable in the wing bending response in the higher range of k values. It is of interest to mention that using the analysis of wind-tunnel wall effects[11] in conjunction with the dimensions of the solid-wall entrance nozzle at the vane location predicts a resonance phenomena on the vanes at k near 0.12. This value corresponds closely to that for the first notch in the data of Figs. 7 and 8. At any rate the dips are believed to be in stream angle, and the need for detailed measurements in this area is apparent. These dips in the response function would probably level out if detailed measurements, such as might be made simultaneously on the model, were available. Further work in this area using hot wire anemometry is continuing.

A comparison of the measured center-of-gravity acceleration response with the calculations for configuration A is shown in Fig. 9. The phase angles are based on the measured phases with the calculated phase of the gust with respect to vane position subtracted (straight lines of Fig. 2c). Although the agreement is only fair, the calculations give the correct trend. Such a result might be expected as a result of the stability derivatives used. Although they were estimated from static force tests of a similar model, there were differences in flexibility levels and fuselage shapes. The model of the force tests also had large engine inlets and internal ducting, whereas the one described herein did not.

Conclusions

From these initial developmental tests of the airstream oscillator, it appears that a means of generating an oscillating airstream of sufficient strength and uniformity for useful gust research has been developed. Also a satisfactory means of mounting the model to simulate the free-flight stability modes is available. The application of this technique should provide a useful means of gust loads research. Several areas that need improvement have become apparent also. Some of these areas are the need for further detailed stream-angle measurements, a more sensitive and simpler technique for measuring stream angle and phase (particularly for use on a model), and streamlining of data acquisition and handling techniques.

Appendix A: Calculation of Frequency-Response Functions for the Rigid-Body Modes, Including the Mount System

The frequency-response functions are calculated based on a stability derivative-type analysis using the equations of motion for pitching and plunging freedoms. The analysis neglects the frequency dependence of the aerodynamics and structural dynamics, but should be satisfactory providing k is not too large, the frequencies of the structural modes are well above the frequencies of the stability modes, and the static margin is not too small.[5] Such analyses have been utilized previously in the gust loads problem for the free-flight case (for example, Refs. 2 and 5). This development essentially extends the previous work to include the mount system springs.

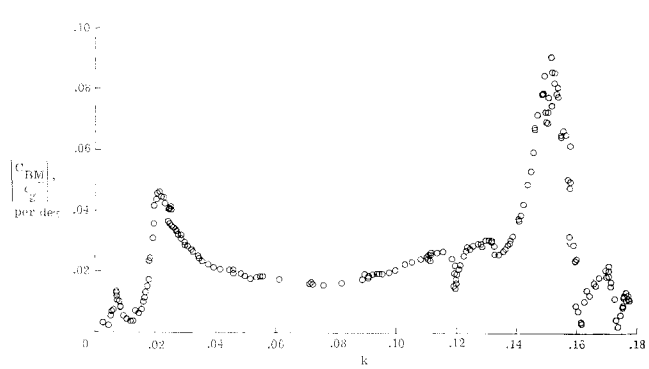

Fig. 7 Measured wing root bending moment amplitude response function for fighter-type model (configuration A) at $M = 1.0$.

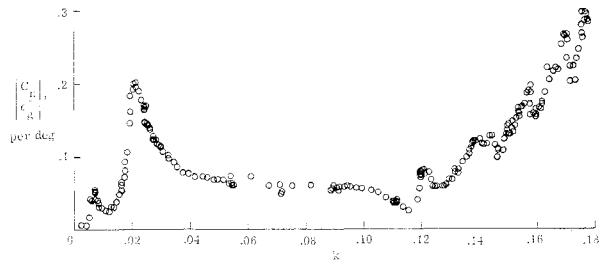

Fig. 8 Measured acceleration response for center of gravity of fighter-type model (configuration A) at $M = 1.0$.

The equations of motion are developed in the same fashion as in Ref. 8, but the angle of attack from trim is substituted as $\alpha = \theta + \dot{z}/V + \epsilon_g$, where ϵ_g is the angle of the oncoming gust referred to the tunnel centerline. The terms involving ϵ_g are considered as forcing functions giving the following equations of motion:

$$\ddot{z} + b_{21}\dot{z} + b_{20}z + c_{20}\theta = d_{20}\epsilon_g$$
$$b_{32}\ddot{z} + b_{31}\dot{z} + b_{30}z + \ddot{\theta} + c_{31}\dot{\theta} + c_{30}\theta = d_{30}\epsilon_g + d_{31}\dot{\epsilon}_g \tag{A1}$$

where

$$\begin{aligned}
b_{21} &= 2\zeta_z(k_{zz}/m)^{1/2} + \sigma(C_{L\alpha} + C_D)\\
b_{20} &= k_{zz}/m\\
b_{32} &= -\tfrac{1}{2}(\sigma/V)(\bar{c}/r_y)^2 C_{m\dot{\alpha}}\\
b_{31} &= -(\sigma/\bar{c})(\bar{c}/r_y)^2 C_{m\alpha}\\
b_{30} &= k_{z\theta}/I_y\\
c_{20} &= k_{z\theta}/m + V\sigma C_{L\alpha}\\
c_{31} &= 2\zeta_\theta(k_{\theta\theta}/I_y)^{1/2} - (\sigma/2)(\bar{c}/r_y)^2(C_{m\dot{\alpha}} + C_{mq})\\
c_{30} &= k_{\theta\theta}/I_y - V(\sigma/\bar{c})(\bar{c}/r_y)^2 C_{m\alpha}\\
d_{20} &= -\sigma V C_{L\alpha}\\
d_{30} &= (\sigma V/\bar{c})(\bar{c}/r_y)^2 C_{m\alpha}\\
d_{31} &= (\sigma/2)(\bar{c}/r_y)^2 C_{m\dot{\alpha}}
\end{aligned} \tag{A2}$$

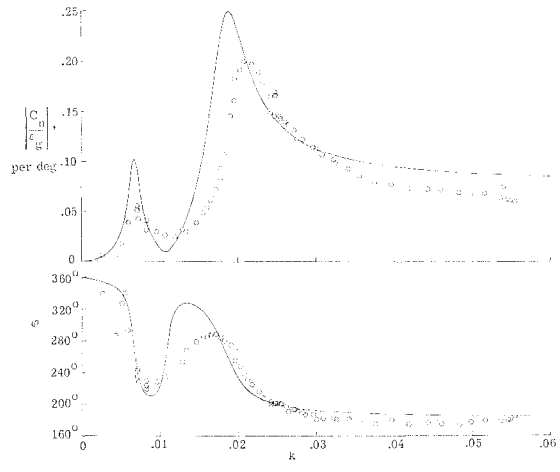

Fig. 9 Comparison of measured and calculated acceleration response for the center of gravity of fighter-type airplane model (configuration A) at $M = 1.0$.

Assuming sinusoidal motion and substituting $z = z_0 e^{i\omega t}$, $\theta = \theta_0 e^{i\omega t}$, and $\epsilon_g = \epsilon_{g_0} e^{i\omega t}$ where z_0, θ_0, and ϵ_{g_0} are complex, gives the following algebraic equations:

$$[(b_{20} - \omega^2) + i\omega b_{21}]z_0 + c_{20}\theta_0 = d_{20}\epsilon_{g_0}$$

$$[(b_{30} - b_{32}\omega^2) + i\omega b_{31}]z_0 + [(c_{30} - \omega^2) + i\omega c_{31}]\theta_0 = (d_{30} + i\omega\, d_{31})\epsilon_{g_0} \quad \text{(A3)}$$

Solving these equations for the ratios z_0/ϵ_{g_0} and θ_0/ϵ_{g_0} and expressing in nondimensional form gives

$$C_n/\epsilon_{g_0} = m\ddot{z}/(qS\epsilon_{g_0}) = m\omega^2/(qS)\{[(C_1 - C_2\omega^2) + i\omega C_3]/[(D_1 - D_2\omega^2 + \omega^4) + i\omega(D_3 - D_4\omega^2)]\} \quad \text{(A4)}$$

$$\theta_0/\epsilon_{g_0} = [(C_5 - C_6\omega^2) + i\omega(C_7 - C_8\omega^2)]/[(D_1 - D_2\omega^2 + \omega^4) + i\omega(D_3 - D_4\omega^2)] \quad \text{(A5)}$$

where

$$\begin{aligned} C_1 &= d_{30}c_{20} - d_{20}c_{30} \\ C_2 &= -d_{20} \\ C_3 &= c_{20}d_{31} - d_{20}c_{31} \\ C_5 &= d_{30}b_{20} - d_{20}b_{30} \\ C_6 &= d_{30} + d_{31}b_{21} - d_{20}b_{32} \\ C_7 &= d_{30}b_{21} + b_{20}d_{31} - d_{20}b_{31} \\ C_8 &= d_{31} \\ D_1 &= b_{20}c_{30} - c_{20}b_{30} \\ D_2 &= b_{20} + c_{30} + b_{21}c_{31} - c_{20}b_{32} \\ D_3 &= b_{20}c_{31} + b_{21}c_{30} - c_{20}b_{31} \\ D_4 &= c_{31} + b_{21} \end{aligned} \quad \text{(A6)}$$

The expressions for k_{zz}, $k_{\theta\theta}$, and $k_{z\theta}$ are given in Ref 8.

Appendix B: Frequency Approximation for Plunging Mode

The characteristic determinant for the longitudinal stability of a model on the cable mount system can be written as[8]

$$\begin{vmatrix} \lambda^2 + b_{21}\lambda + b_{20} & c_{20} \\ b_{32}\lambda^2 + b_{31}\lambda + b_{30} & \lambda^2 + c_{31}\lambda + c_{30} \end{vmatrix} = 0 \quad \text{(B1)}$$

where λ is the exponent in a solution of the form $e^{\lambda t}$ and the coefficients are defined by Eq. (A2). The frequency of the plunging mode is generally much less than the basic pitch frequency such that the static approximation to pitching motion can be made by neglecting $\lambda^2 + c_{31}\lambda$ in the lower right-hand element. Furthermore, b_{32} is generally small and can be neglected. Expanding the determinant then gives the characteristic equation

$$\lambda^2 + (b_{21} - b_{31}c_{20}/c_{30})\lambda + (b_{20} - b_{30}c_{20}/c_{30}) = 0 \quad \text{(B2)}$$

The undamped natural frequency is

$$\omega_p^2 = b_{20} - b_{30}c_{20}/c_{30} \quad \text{(B3)}$$

Substitution from Eq. (A2) gives the following expression:

$$\omega_p^2 = (k_{zz}/m)\{1 - (k_{z\theta}/k_{zz})[qSC_{L\alpha}/(k_{\theta\theta} - qS\bar{c}C_{m\alpha})]\} \quad \text{(B4)}$$

This equation gives a good approximation to the plunging mode frequency over a wide range of cable tension.

The corresponding expression for the damping does not give a satisfactory approximation to the stability boundary. It indicates that the plunging mode could be unstable only for $C_{m\alpha} > 0$; however, instability can be encountered for $C_{m\alpha} < 0$. Furthermore, the next approximation, which would include $b_{31}\lambda$ and result in a cubic characteristic equation, yields a similar conclusion (from Routh's discriminant). This implies that the complete quartic should be used in investigating the stability boundary for this mode.

References

[1] Houbolt, J. C., Steiner, R., and Pratt, K. G., "Dynamic response of airplanes to atmospheric turbulence including flight data on input and response," NASA TR R-199 (1964).

[2] Bennett, F. V. and Pratt, K. G., "Calculated responses of a large swept-wing airplane to continuous turbulence with flight-test comparisons," NASA TR R-69 (1960).

[3] Coleman, T. L., Press, H., and Meadows, M. T., "An evaluation of effects of flexibility on wing strains in rough air for a large swept-wing airplane by means of experimentally determined frequency-response functions with an assessment of random-process techniques employed," NASA TR R-70 (1960).

[4] Chernoff, M. and Rothman, H. L., "Unsteady frequency response functions for use in power spectral analysis," J. Aerospace Sci. **29**, 121–129 (1962).

[5] Zbrozek, J. K., "Longitudinal response of aircraft to oscillatory vertical gusts (frequency analysis including the effect of unsteady aerodynamics)," British Royal Aircraft Establishment Rept. Aero. 2559 (1955).

[6] Hakkinen, R. J. and Richardson, A. S., Jr., "Theoretical and experimental investigation of random gust loads. Part I—Aerodynamic transfer function of a simple wing configuration in incompressible flow," NACA TN 3878 (1957).

[7] Reid, C. F., Jr. and Wrestler, C. G., Jr., "An investigation of a device to oscillate a wind-tunnel airstream," NASA TN D-739 (1961).

[8] Reed, W. H., III and Abbott, F. T., Jr., "A new free-flight mount system for high speed wind-tunnel flutter models," Proceedings of the Symposium on Aeroelastic Dynamic Modeling Technology, U.S. Air Force Systems Command, RTD-TDR-63-4197, Pt. I (1964).

[9] Yates, E. C., Jr. and Fox, A. G., "Steady-state characteristics of a differential pressure system for evaluating angles of attack and sideslip of the Ranger IV vehicle," NASA TN D-1966 (1963).

[10] Reed, W. H., III, Hall, A. W., and Barker, L. E., Jr., "Analog techniques for measuring the frequency response of linear physical systems excited by frequency-sweep inputs," NASA TN D-508 (1960).

[11] Runyan, H. L., Woolston, D. S., and Rainey, A. G., "Theoretical and experimental investigation of the effect of tunnel walls on the forces on an oscillating airfoil in two-dimensional subsonic compressible flow," NACA Rept. 1262 (1956).